


Conserved Sequence Preferences Contribute to Substrate Recognition by the Proteasome*^[S]

Received for publication, March 23, 2016, and in revised form, May 16, 2016. Published, JBC Papers in Press, May 17, 2016, DOI 10.1074/jbc.M116.727578

Houqing Yu^{†‡§}, Amit K. Singh Gautam[‡], Shameika R. Wilmington^{†§}, Dennis Wylie[¶], Kirby Martinez-Fonts^{‡§}, Grace Kago[‡], Marie Warburton[‡], Sreenivas Chavali^{||}, Tomonao Inobe^{**}, Ilya J. Finkelstein[‡], M. Madan Babu^{||1}, and  Andreas Matouschek^{†‡§2}

From the [†]Department of Molecular Biosciences and the [¶]Center for Computational Biology and Bioinformatics, The University of Texas at Austin, Austin, Texas 78712, the [§]Department of Molecular Biosciences, Northwestern University, Evanston, Illinois 60208, the ^{||}Medical Research Council, Laboratory of Molecular Biology, Cambridge CB2 0QH, United Kingdom, and ^{**}Frontier Research Core for Life Sciences, University of Toyama, 3190 Gofuku, Toyama-shi, Toyama 930-8555, Japan

The proteasome has pronounced preferences for the amino acid sequence of its substrates at the site where it initiates degradation. Here, we report that modulating these sequences can tune the steady-state abundance of proteins over 2 orders of magnitude in cells. This is the same dynamic range as seen for inducing ubiquitination through a classic N-end rule degron. The stability and abundance of His3 constructs dictated by the initiation site affect survival of yeast cells and show that variation in proteasomal initiation can affect fitness. The proteasome's sequence preferences are linked directly to the affinity of the initiation sites to their receptor on the proteasome and are conserved between *Saccharomyces cerevisiae*, *Schizosaccharomyces pombe*, and human cells. These findings establish that the sequence composition of unstructured initiation sites influences protein abundance *in vivo* in an evolutionarily conserved manner and can affect phenotype and fitness.

The proteasome controls the concentrations of thousands of regulatory proteins, removes misfolded and damaged proteins in cells, and digests foreign proteins to produce peptides that are displayed by the major histocompatibility complex (MHC) at the cell surface (1, 2). Proteins are targeted to the proteasome by ubiquitin chains, but these chains also have other biological functions (3, 4). The pattern through which ubiquitin moieties are linked and their number in the chains convey some targeting specificity. For example, chains of four or more ubiquitin

moieties linked through Lys-48 of ubiquitin are thought to be the canonical proteasome targeting signal (5), whereas short tags of one ubiquitin or chains linked through Lys-63 are associated with membrane trafficking (6–8) and DNA repair (9).

Recent research shows that a much broader spectrum of ubiquitin linkages is associated with proteasome degradation (10, 11). In other cases, the same ubiquitin linkage can target proteins to different cellular processes (2, 3, 12–18). Even ubiquitin-tagged proteins that are recognized by the proteasome are not always degraded. It has been proposed that competition between different ubiquitin receptors (19) can protect some ubiquitinated proteins from proteasomal degradation. Additionally, disassembly of some polyubiquitin chains by specialized deubiquitinating enzymes on the proteasome can inhibit degradation (20).

Targeting information may also be encoded directly in the substrate protein itself. Efficient degradation requires the presence of an unstructured or disordered region in the substrate protein. The proteasome engages the substrate's disordered region to initiate unfolding and translocation to the proteolytic sites (21–24). The selection of the initiation site by the proteasome is part of the mechanism that confers specificity to degradation (25–28). Indeed, the absence of proteasomal initiation sites explains the unexpected stability of several natural proteins in yeast, such as the ubiquitin-conjugating enzyme Cdc34 and the proteasomal shuttle receptor Rad23 (27, 28). The requirement of initiation sites for degradation is also reflected in the half-lives of proteins measured in large scale proteomics experiments on yeast and mammalian cells (23, 28, 29). Proteins that contain predicted proteasome initiation regions have shorter half-lives than proteins that lack these regions (23, 28).

We recently investigated the proteasome's preferences for the amino acid sequence of its initiation sites *in vitro* by comparing the rates by which purified yeast proteasomes degraded a series of model proteins (28). However, it is possible that the proteasome's intrinsic preferences are overridden *in vivo*. For example, regulatory proteins such as p97/Cdc48/VCP may deliver already unfolded proteins to the proteasome (30–36). These considerations raise several questions. Are the initiation sequence preferences identified *in vitro* operational *in vivo*? If so, do the preferences affect protein abundance substantially and influence phenotype and cell fitness? How does the magnitude of the effect compare with that achieved by the regulation

* This work was supported in part by National Institutes of Health Grants U54GM105816, R21CA196456, and R21CA191664 (to A. M.), Welch Foundation Grants F-1817 (to A. M.) and F-1808 (to I. J. F.), Cancer Prevention and Research Institute of Texas Grant RP140328 (to A. M.), the Program to Disseminate Tenure Track System from the Ministry of Education, Culture, Sports, Science and Technology, Japan (to T. I.), the United Kingdom Medical Research Council Grant MC_U105185859 (to M. M. B.), and the European Molecular Biology Organization Long-Term Fellowship (to S. C.) and Young Investigator Program (to M. M. B.). The authors declare that they have no conflicts of interest with the contents of this article. The content is solely the responsibility of the authors and does not necessarily represent the official views of the National Institutes of Health.

✂ Author's Choice—Final version free via Creative Commons CC-BY license.

^[S] This article contains supplemental Tables S1–S3.

¹ Lister Institute Research Prize Fellow.

² To whom correspondence should be addressed: Dept. of Molecular Biosciences, The University of Texas at Austin, 2506 Speedway Stop A5000, Austin, TX 78712. Tel.: 512-232-4045; Fax: 512-471-1218; E-mail: matouschek@austin.utexas.edu.

Sequence Preferences in Proteasome Degradation

of ubiquitination? Are the sequence preferences for the initiation site conserved in different organisms?

Here, we investigate whether the proteasome has sequence preferences in cells using a scalable assay to monitor protein stability. We find that changes in the initiation sequence in model proteasome substrates tune protein degradation rates and adjust protein steady-state abundance over 2 orders of magnitude. These differences in abundance correspond to the dynamic range that is achieved by controlling ubiquitination. Modulating proteasomal initiation can change protein abundance sufficiently to affect cellular fitness by targeting His3 protein to degradation. We observe that the proteasome's sequence preferences are conserved between *Saccharomyces cerevisiae*, *Schizosaccharomyces pombe*, and cultured human cells (HEK293 cells). The sequence preferences reflect the binding affinity of the initiation regions to their recognition site on the proteasome and are related to specific physical and chemical properties of the amino acid sequences.

Results

Monitoring Proteasomal Degradation in Vivo—To investigate protein targeting to the proteasome in *S. cerevisiae*, we assayed the abundance of fluorescent proteasome substrates by measuring total cell fluorescence. We constructed YFP variants with or without different degradation signals or degrons and expressed them from the constitutive *tpi1* promoter (37) on a CEN plasmid in *S. cerevisiae*. To correct for differences in plasmid copy number, transcription and translation levels, and cell size, we also expressed the RFP³ dsRed-Express2 (38) from a constitutive *pgk1* promoter (37) on the same plasmid (Fig. 1, A and B). The ratio of YFP over RFP fluorescence of individual cells served as a measure of the steady-state concentration of the YFP variants (39, 40). A high numerical value of the ratio of yellow fluorescence intensity to red fluorescence intensity (high YFP/RFP ratio) reports high YFP protein abundance and thus inefficient proteasomal degradation, and vice versa.

We targeted YFP to the proteasome by attaching the UbL domain of yeast Rad23 to its N terminus. The UbL domain is recognized by receptors on the proteasome (41–43), but the UbL domain and YFP lack disordered regions at which the proteasome can initiate degradation so that the UbL-YFP protein accumulated in cells and was easily detected by flow cytometry (Fig. 1B). Treating the cells with bortezomib, which partially inhibits the proteasome in *S. cerevisiae* (44, 45), did not increase UbL-YFP levels noticeably (Fig. 1B). Attaching a 51-residue C-terminal tail derived from subunit 9 of the *F_o* component of the *Neurospora crassa* ATP synthase (Su9, sequence P in supplemental Table S1) to UbL-YFP reduced the yellow cell fluorescence to low levels slightly above the background fluorescence of cells not expressing YFP (Fig. 1B), suggesting that the UbL-YFP-Su9 protein was degraded efficiently. The red fluorescence of the RFP reference protein was not affected significantly (Fig. 1B). In the presence of bortezomib, UbL-YFP-Su9 fluorescence increased, showing that degradation depends on the proteasome, but to levels lower than UbL-YFP, as expected

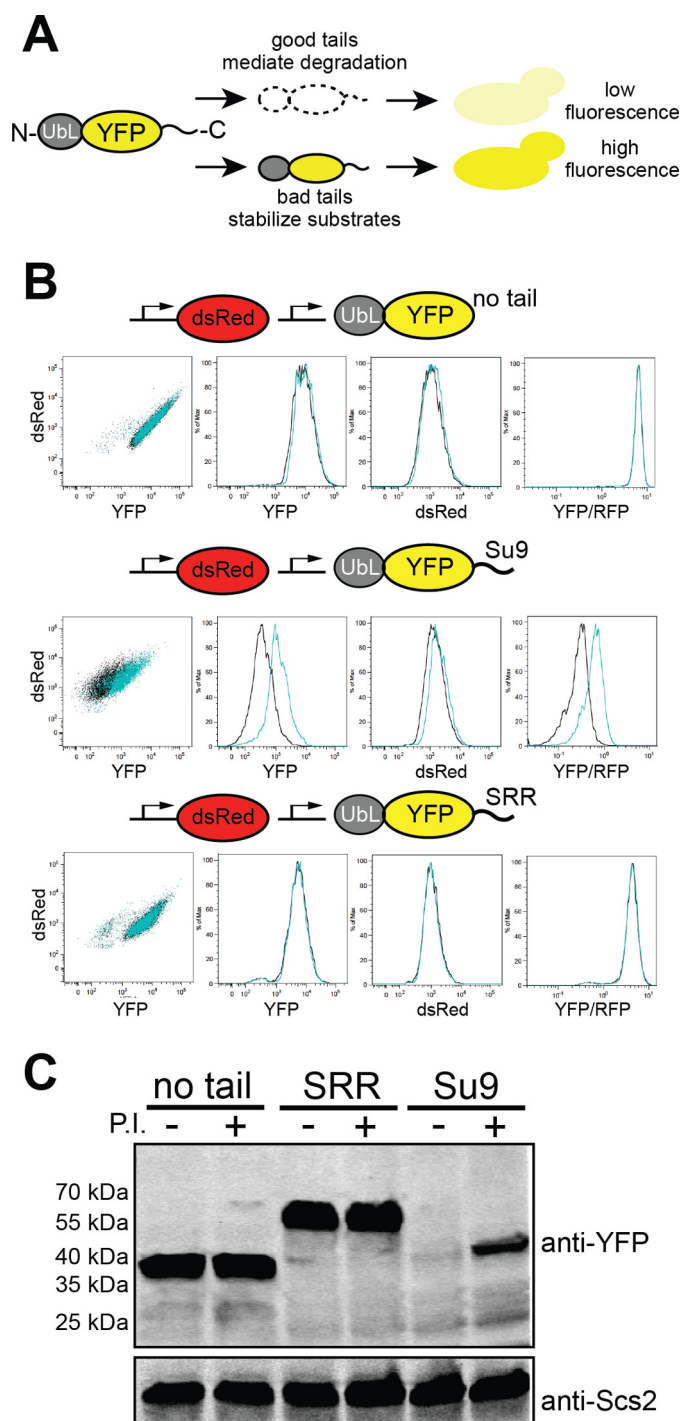


FIGURE 1. Assessing proteasomal initiation in *S. cerevisiae*. A, outline of the fluorescence-based degradation assay in *S. cerevisiae*. Proteasome substrates consisted of an N-terminal UbL domain derived from *S. cerevisiae* Rad23, followed by a YFP domain, and finally a disordered tail at the C terminus. Tails that allow the proteasome to initiate degradation resulted in a low cellular YFP signal, whereas tails that are not recognized by the proteasome led to a high YFP signal. B, cell fluorescence profiles of *S. cerevisiae* cultures expressing proteasome substrates with different initiation sequences monitored by flow cytometry. Cells were treated with proteasome inhibitor (100 μ M bortezomib, cyan population) or DMSO (black population). 10,000 cells were collected in each flow cytometry run. C, cellular abundance of YFP substrates (UbL-YFP-tail) without an initiation sequence (no tail, Q) or with poor (SRR tail, E in supplemental Table S1) or effective (Su9 tail, P in supplemental Table S1) initiation sequences was assayed by Western blotting. The proteasome was inhibited with 100 μ M bortezomib where indicated; the integral endoplasmic reticulum membrane protein Scs2, detected with a specific Scs2 antibody, served as the loading control.

³ The abbreviations used are: RFP, red fluorescent protein; DHFR, dihydrofolate reductase; 3-AT, 3-amino-1,2,4-triazole; IQR, interquartile range.

Sequence Preferences in Proteasome Degradation

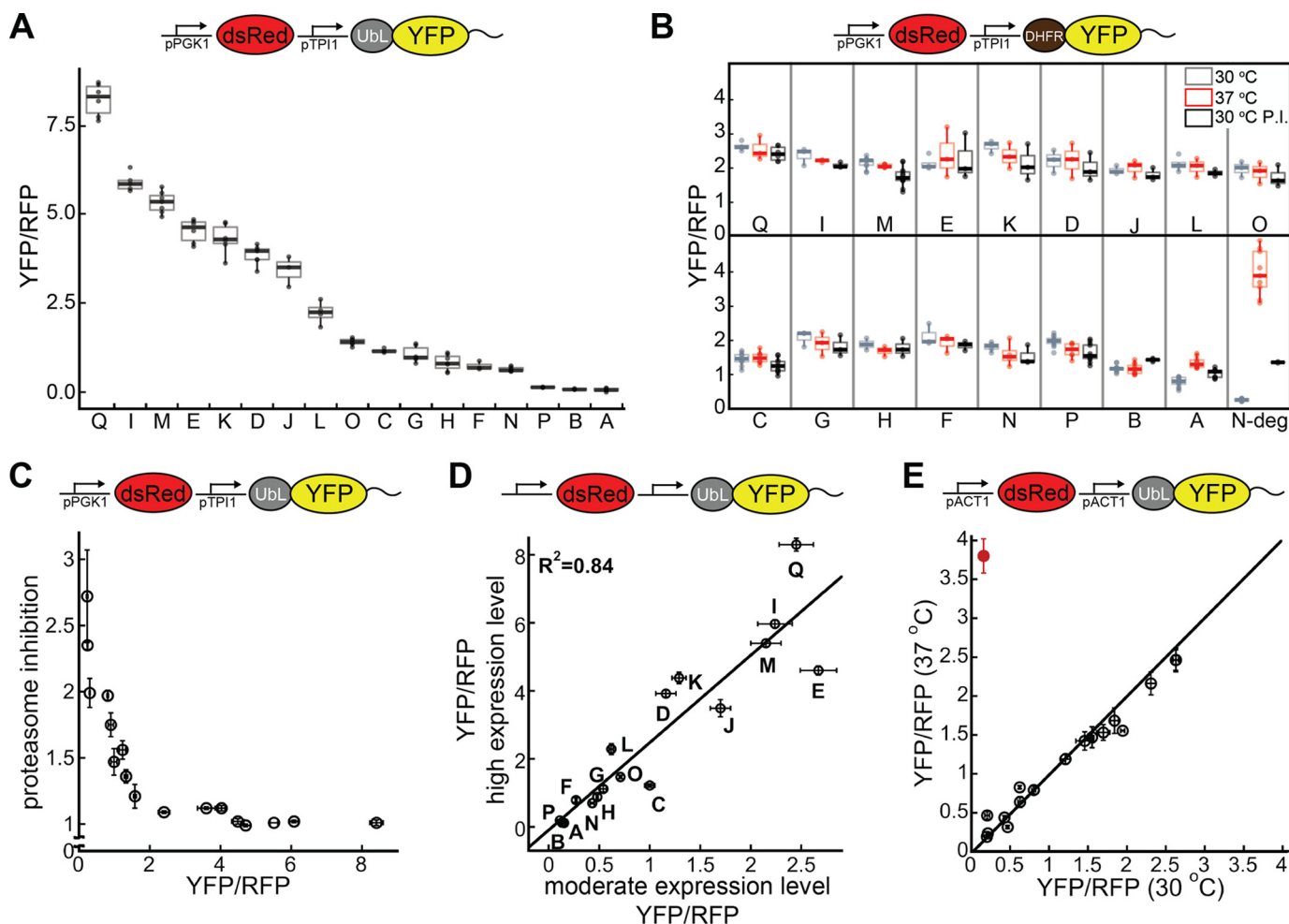


FIGURE 2. Proteasomal preferences for initiation sequences in *S. cerevisiae*. *A*, boxplots of corrected median cellular YFP fluorescence (median YFP/RFP values) for cultures expressing fluorescent proteasome substrates with different tails at their C termini (pPGK1 dsRed, pTPI1 UbL-YFP-tail; tail sequences shown in supplemental Table S1). Whiskers contain data within 1.5 interquartile range (IQR) of box. The IQR of the data is the difference between the 3rd quartile (75th percentile) and 1st quartile (25th percentile) and thus corresponds to the height of the box. *B*, boxplots (1.5 IQR whiskers) of YFP/RFP values for proteasome substrates in which the UbL domain was replaced with a DHFR domain (DHFR-YFP-tail) in the E1 temperature-sensitive strain *uba1-204* at the permissive (30 °C, gray) and restrictive (37 °C, red) temperatures and after proteasome inhibition (30 °C + 100 μ M bortezomib, black). *N-deg*, YFP substrate with N-end rule degen. *C*, graph plots median YFP/RFP values upon proteasome inhibition against the YFP/RFP values of each proteasome substrate. The recovery was calculated as the ratio of the median YFP/RFP values for cultures grown after addition of 100 μ M bortezomib and DMSO. For stable YFP proteins, the YFP/RFP value does not change upon proteasome inhibition (recovery \approx 1), and for well degraded proteins, the YFP/RFP value recovers as the proteasome is inhibited (recovery $>$ 1). *D*, graph plots median YFP/RFP values for cell cultures expressing proteasome substrates expressed at high levels (pPGK1 dsRed, pTPI1 UbL-YFP-tail) against the median YFP/RFP values for the same protein expressed at moderate levels (pACT1 dsRed, pACT1 UbL-YFP-tail). The correlation coefficient is calculated for a fit to a straight line. *E*, median YFP/RFP values of cell cultures expressing proteasome substrates with different tails at their C termini at moderate expression levels (pACT1 dsRed, pACT1 UbL-YFP-tail, black circles) in the E1 temperature-sensitive strain *uba1-204* at the permissive (30 °C) or the restrictive (37 °C) temperature. A ubiquitination-dependent N-end rule substrate is also shown (Ub-R-KK-YFP-Su9, red circle). The median YFP/RFP values for each construct were calculated from 10,000 cells collected in one flow cytometry run. Data points in panels *C*, *D*, and *E* represent mean values determined from at least three repeat experiments; error bars indicate S.E.

if proteasome inhibition is incomplete (Fig. 1*B*). Analysis of cell extracts by SDS-PAGE and Western blotting confirmed that the UbL-YFP-Su9 protein was depleted from cells in a proteasome-dependent manner and that the protein was degraded completely as no partially degraded protein fragments could be detected (Fig. 1*C*). Replacing the Su9 tail with a sequence consisting almost entirely of Ser residues (serine-rich region or SRR, sequence E in supplemental Table S1) stabilized the protein and restored UbL-YFP-SRR levels almost to those seen for UbL-YFP without an initiation region (Fig. 1*B*). Proteasome inhibition by bortezomib did not cause further increase in UbL-YFP-SRR levels (Fig. 1, *B* and *C*). These results show that only some disordered tails allow the proteasome to initiate degradation in cells.

Initiation Sequence Preferences in Vivo—Next, we fused UbL-YFP to 14 additional disordered C-terminal tails (supplemental Table S1) and used the fluorescence assay described above to investigate intracellular degradation. The steady-state abundance of these proteins, as judged by YFP/RFP ratios, varied \sim 70-fold between the most and least stable proteins (Fig. 2*A* and Table 1).

Degradation of the YFP proteins depended on the UbL domain and was not due to ubiquitination of the disordered tails. *S. cerevisiae* encodes only one ubiquitin-activating enzyme (46), Uba1, and the temperature-sensitive *uba1-204* allele makes it possible to reduce protein ubiquitination substantially by shifting cells to the restrictive temperature (47). We replaced the UbL domain with a DHFR domain and fused

TABLE 1

YFP/RFP ratios of constructs in *S. cerevisiae*, *S. pombe*, and mammalian cells (HEK293)

The median of YFP/RFP ratio for each construct was calculated from 10,000 cells collected in one flow cytometry run and used to indicate the abundance of the YFP substrate in yeast cells as described under "Experimental Procedures." Data represent mean values and standard errors determined from at least three repeat experiments. ND is not determined; NS indicates derived from influenza A virus non-structural protein 1 (NS1); GRR indicates glycine-rich region (derived from human p105); NB indicates derived from influenza B virus glycoprotein NB; SNS indicates tandem repeat of SP2-NB-SP2; NBS indicates tandem repeat of NB-NB-SP2; DRR indicates aspartic acid (D)-rich region (derived from *S. cerevisiae* Cdc34); SP1 indicates peptide region 1 in influenza A virus M2 protein used to produce antisera; SP2 indicates peptide region 2 in influenza A virus M2 protein used to produce antisera; SPmix indicates tandem repeat of SP1 and SP2 (SP2-SP1-SP2-SP1-SP2); PEST indicates sequence from human IκBα; SRR indicates serine-rich region (derived from herpes virus 1 ICP4); Su9, derived from subunit 9 of *N. crassa* ATP synthase component F_0 ; eRR, derived from *E. coli* lacI; ODC indicates derived from ornithine decarboxylase; 35 indicates derived from *S. cerevisiae* cytochrome b_2 .

Tail	Name	<i>S. cerevisiae</i>			<i>S. pombe</i>	HEK293
		pACT1 UbL-YFP-tail pACT1 dsRed	pTPI1 UbL-YFP-tail pPGK1 dsRed	pTPI1 UbL-GFP-tail pPGK1 dsRed		
A	35	0.15 ± 0.01	0.12 ± 0.02	0.13 ± 0.01	0.73 ± 0.06	0.20 ± 0.02
B	ODC	0.13 ± 0.01	0.13 ± 0.01	0.034 ± 0.004	1.0 ± 0.3	0.13 ± 0.02
C	Poly(G)	1.00 ± 0.05	1.22 ± 0.05	1.07 ± 0.08	ND	0.51 ± 0.01
D	GRR	1.2 ± 0.1	3.9 ± 0.1	1.9 ± 0.1	4.8 ± 0.2	0.83 ± 0.05
E	SRR	2.7 ± 0.2	4.6 ± 0.1	3.81 ± 0.09	6.54 ± 0.07	0.87 ± 0.02
F	NB	0.27 ± 0.01	0.79 ± 0.07	0.27 ± 0.02	2.8 ± 0.2	0.31 ± 0.02
G	NS	0.54 ± 0.03	1.12 ± 0.09	0.80 ± 0.03	2.3 ± 0.1	0.27 ± 0.02
H	SP1	0.48 ± 0.01	0.88 ± 0.08	0.63 ± 0.01	3.0 ± 0.1	0.47 ± 0.03
I	SP2	2.2 ± 0.2	6.0 ± 0.1	4.30 ± 0.06	5.65 ± 0.07	0.86 ± 0.04
J	SPmix	1.7 ± 0.1	3.5 ± 0.3	2.40 ± 0.07	5.94 ± 0.09	0.834 ± 0.004
K	SNS	1.29 ± 0.07	4.4 ± 0.2	2.7 ± 0.2	4.77 ± 0.07	0.70 ± 0.02
L	NBS	0.62 ± 0.02	2.3 ± 0.2	1.01 ± 0.07	5.2 ± 0.1	0.54 ± 0.02
M	DRR	2.2 ± 0.2	5.4 ± 0.1	4.6 ± 0.3	4.9 ± 0.2	0.76 ± 0.03
N	eRR	0.43 ± 0.02	0.70 ± 0.02	0.40 ± 0.01	1.10 ± 0.05	0.28 ± 0.02
O	PEST	0.71 ± 0.01	1.47 ± 0.04	0.98 ± 0.08	2.85 ± 0.08	0.21 ± 0.01
P	Su9	0.11 ± 0.03	0.19 ± 0.01	0.14 ± 0.02	1.7 ± 0.2	0.16 ± 0.01
Q	No tail	2.5 ± 0.2	8.3 ± 0.2	5.1 ± 0.3	6.8 ± 0.1	0.83 ± 0.06

the DHFR-YFP variants to the same 16 tails in a *uba1-204* strain. The steady-state levels of 14 of these proteins were similar both at the restrictive temperature and at the permissive temperature in the absence or presence of bortezomib (Fig. 2C). Shifting the *uba1-204* strain to the restrictive temperature does inhibit ubiquitin-dependent degradation of YFP substrate with a classic N-end rule degron (see below) more than 20-fold (Fig. 2B). These results indicate that most DHFR-YFP-tail variants are neither ubiquitinated nor degraded by the proteasome. The steady-state level of DHFR-YFP-35, which has a tail derived from the pre-sequence of *S. cerevisiae* cytochrome b_2 (sequence A in supplemental Table S1), increased at the restrictive temperature and at the permissive temperature in the presence of bortezomib (Fig. 2C), suggesting that this sequence did become ubiquitinated to some extent. The steady-state level of DHFR-YFP-ODC, which has a tail derived from the 37 C-terminal amino acids of ornithine decarboxylase (sequence B in supplemental Table S1), increased by a small amount at the permissive temperature in the presence of bortezomib but was not ubiquitin-dependent (Fig. 2B). Proteasomal degradation of ornithine decarboxylase is known to be ubiquitin-independent (48, 49), suggesting that DHFR-YFP-ODC is directly targeted to the proteasome by the ODC tail. However, UbL-YFP-ODC was degraded substantially more efficiently than DHFR-YFP-ODC (Fig. 2, A and B), showing that tethering to the proteasome is important for robust degradation.

Inhibiting the proteasome with bortezomib increased accumulation of the least stable proteins by ~3-fold, had no effect on the most stable proteins, and affected the proteins in-between proportionally to their abundance (Fig. 2C). Thus, degradation of unstable UbL-YFP-tail proteins was by the proteasome.

In principle, promoter strength might influence the proteasomal degradation of different proteins via aggregation or sat-

uration of the folding or degradation machinery. To test this possibility, we expressed the set of UbL-YFP variants as well as RFP reference protein from two *act1* promoters (50) on the same CEN plasmid, which reduced cellular levels of a non-degraded UbL-YFP protein ~5-fold compared with expression from the *tpi1* promoter (data not shown). At these lower expression levels, there was a 25-fold difference in abundance between proteins that degraded effectively (e.g. UbL-YFP-Su9; sequence P) and the proteins that degraded poorly (e.g. UbL-YFP-SRR; sequence E) (Table 1 and Fig. 2, D and E). Importantly, the steady-state levels of the UbL-YFP-tail proteins expressed from stronger and weaker promoters were highly correlated ($R^2 = 0.84$; Fig. 2D). Thus, different expression levels did not cause a significant difference in the contribution of the tails to the initiation of proteasomal degradation. Again, degradation depended on the UbL domain and the proteasome (data not shown) and was not affected by ubiquitination, except for UbL-YFP-35 (sequence A in supplemental Table S1; Fig. 2E). UbL-YFP-35 was stabilized ~2-fold when ubiquitination was inhibited, compared with a 25-fold stabilization when the tail was removed. Thus, the 35 tail was ubiquitinated to some extent, but its ubiquitination made a relatively small contribution to proteasome targeting.

Proteasome Initiation Tunes Degradation over a Similar Range as Ubiquitination—Next, we asked whether initiation regions could modulate proteasomal degradation over the same dynamic range as achieved through the regulation of ubiquitination of a classic degron. We replaced the UbL domain of UbL-YFP-Su9 with an N-end rule degron consisting of a ubiquitin domain followed by a destabilizing (Arg) or stabilizing (Val) residue and a linker derived from *Escherichia coli* lacI, which contains two Lys residues (51, 52). In the cell, the ubiquitin domain is cleaved off by ubiquitin hydrolases, and an Arg residue leads to ubiquitination of the degron but a Val does not.

Sequence Preferences in Proteasome Degradation

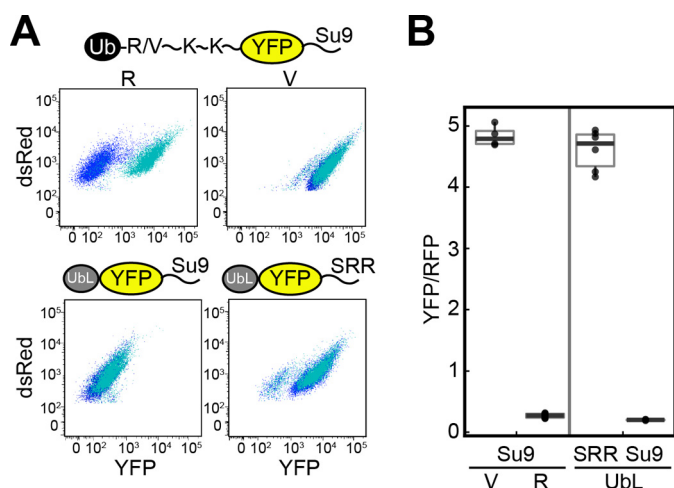


FIGURE 3. Proteasome initiation tunes protein abundance over a similar range as ubiquitination. *A*, cell fluorescence profiles of *S. cerevisiae* cultures expressing UbL-YFP-tail and N-end rule substrates. *Top row*, cells expressing N-end rule degron substrates with a destabilizing residue as the N degron (Ub-R-KK-YFP-Su9) or a stabilizing residue as the N degron (Ub-V-KK-YFP-Su9); *bottom row*, cells expressing UbL-YFP proteins with a tail that serves as an effective proteasome initiation site (Su9; P in supplemental Table S1) or a poor proteasome initiation site (SRR; E in supplemental Table S1). The proteins were expressed in the E1 temperature-sensitive strain *uba1-204* at the permissive temperature (30 °C, blue) or the restrictive temperature (37 °C, cyan). *B*, boxplots (1.5 IQR whiskers) of corrected YFP fluorescence (median YFP/RFP values) for cells expressing the N-end rule substrates and UbL substrates analyzed in *A*. The median YFP/RFP value for each construct was calculated from 10,000 cells collected in one run in flow cytometry.

Steady-state levels of the R-KK-YFP-Su9 protein were low and similar to those of UbL-YFP-Su9 (Fig. 3*A*, blue populations), whereas levels of the V-KK-YFP-Su9 protein were high and similar to those of UbL-YFP-SRR (Fig. 3*A*, blue populations). Inhibiting ubiquitination by shifting *uba1-204* cells to the restrictive temperature increased protein levels for R-KK-YFP-Su9 but did not affect V-KK-YFP-Su9, UbL-YFP-Su9 or UbL-YFP-SRR levels (Fig. 3*A*, cyan populations). Altering the N-end rule degron from Arg to Val changed YFP levels ~26-fold (Fig. 3*B*), whereas modulating initiation by replacing the Su9 tail of UbL-YFP-Su9 with an SRR tail changed YFP fluorescence ~24-fold (Fig. 3*B*). Thus, the identity of the initiation region can be as important as the regulation of ubiquitination in targeting proteins to proteasomal degradation.

Steady-state Levels Correlate with Degradation Rates—The steady-state abundance of UbL-YFP-tail variants depended on the rates at which they were degraded by the proteasome in the cell. We measured degradation rates by inhibiting protein synthesis with cycloheximide and measured the amount of YFP substrate remaining over time (Fig. 4*A*). The half-lives of YFP substrates with different tails correlated well ($R^2 = 0.76$) with their steady-state levels (Fig. 4*B*). The half-lives also varied over a similar dynamic range as the steady-state levels, with the least stable protein being degraded 68-fold faster than the most stable protein (Table 2). Thus, altering proteasomal initiation by changing the amino acid sequence of the disordered tails can tune degradation rates in the cell over a wide dynamic range. We conclude that the steady-state accumulation of the different proteins reflected the rates with which they were degraded by the proteasome.

We also measured degradation rates for a subset of UbL-YFP-tail proteins by expressing them from a *gal1* promoter (37) and then shutting off expression by adding glucose. The rate constants determined in these experiments were very similar to the rate constants measured in the cycloheximide shut-off experiments for the same proteins expressed from the strong *tpi1* promoter (Fig. 4*C*).

Proteasomal Sequence Preferences Are Consistent for Different Proteins and Can Affect Fitness—Next, we tested whether altering proteasomal initiation of degradation could regulate the abundance of proteins other than YFP. We first replaced the YFP domain of UbL-YFP-tail proteins with jellyfish green fluorescent protein (GFP) (53), and found that the cellular levels of the UbL-GFP-tail and UbL-YFP-tail proteins were affected by the tail sequences in similar ways ($R^2 = 0.94$ for a linear fit, Table 1).

Fluorescent proteins do not occur naturally in *S. cerevisiae*, and their overexpression can have pleiotropic effects (50). To test a different protein, we chose *S. cerevisiae* His3, which is required for growth in medium lacking histidine (54). We constructed UbL-His3-tail proteins (Fig. 5) with the same 16 initiation regions analyzed in the YFP constructs, as well as a UbL-His3 protein without a tail and two His3 variants in which the UbL domain was replaced with a DHFR domain (DHFR-His3 and DHFR-His3-Su9). We tested whether expressing these proteins could complement growth of a *his3* mutant strain, using a competitive inhibitor of His3 (3-AT) to enhance assay sensitivity (55). Yeast with the parental control vector did not grow in the absence of histidine, but strains expressing the His3 variants that are not expected to be degraded, namely UbL-His3, DHFR-His3, and DHFR-His3-Su9, restored growth (Fig. 5*B*).

The growth phenotypes of the 16 different strains expressing UbL-His3-tail proteins fell into three broad groups, robust complementation, modest complementation, and poor or no complementation (Fig. 5*B*). The initiation sequences in the tails that prevented UbL-His3-tail proteins to complement in this assay also resulted in rapid degradation of the corresponding UbL-YFP-tail proteins. The tails that gave modest complementation resulted in intermediate UbL-YFP-tail degradation rates, and the tails that fully complemented resulted in slow degradation of UbL-YFP-tail proteins (*cf.* Figs. 2*A* and 4*A* with 5*B*). Expression of the His3 fusion proteins was not deleterious to yeast cells because supplementing the medium with histidine restored wild-type growth (Fig. 5*B*). In summary, the proteasome shows distinct preferences for the sequence of the disordered region in its substrate where it initiates degradation. These preferences are not dependent on the nature of the protein that is degraded. Furthermore, regulation of protein degradation by modulation of proteasome initiation can affect cell fitness.

Initiation Sequence Preferences Are Similar in Different Organisms—The proteasome is evolutionarily conserved (56), although its processivity can vary substantially between different organisms (57). This raises the question whether the initiation rules for proteasomal degradation are the same for different organisms. To address this question, we tested the degradation of UbL-YFP-tail proteins in *S. pombe* and in cul-

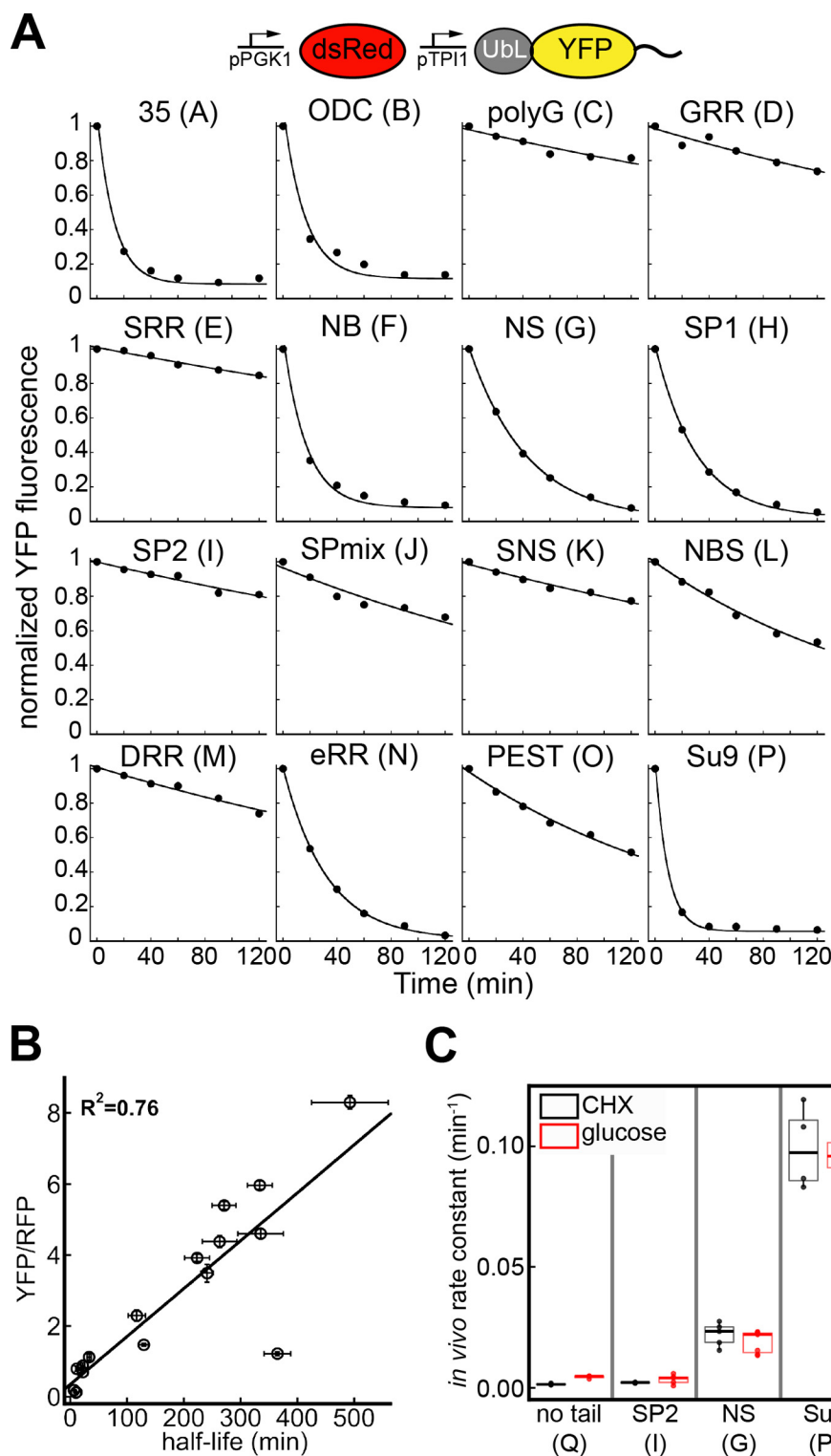


FIGURE 4. Steady-state protein abundances correlate with degradation rates. *A*, normalized time courses of YFP fluorescence illustrating *in vivo* degradation of UbL-YFP-tail constructs for 16 different tails after inhibition of protein synthesis by the addition of $125 \mu\text{M}$ cycloheximide. *Graphs* show one representative dataset of at least three independent experiments. *B*, relationship between protein abundance and half-life in yeast. The steady-state YFP/RFP ratios of fluorescent substrates with 16 different tails are plotted against the half-lives determined by nonlinear fitting of the data shown in *A* to a single exponential decay. The correlation coefficient is calculated for a fit to a straight line. Data points represent mean values determined from at least three repeat experiments; *error bars* indicate S.E. *C*, degradation rate constants of YFP substrates in yeast obtained from the cycloheximide chase experiment in *A* (*black*) and from a glucose shutdown assay (*red*) are shown. The median cellular YFP fluorescence for each construct at each time point was calculated from 10,000 cells collected in one run in flow cytometry; repeat experiments yielded the median values indicated in the *boxplots* shown (1.5 IQR whiskers).

Sequence Preferences in Proteasome Degradation

TABLE 2

Binding affinities of initiation sequences to the proteasome and *in vivo* degradation rate constants of fluorescent substrates (Ubl-YFP-tail) in yeast

See Table 1 for definitions of names.

Name	K_i	<i>In vivo</i> degradation rate constant	
		μM	min^{-1}
35	36 ± 6		0.071 ± 0.004
ODC	28 ± 3		0.068 ± 0.007
Poly(G)			0.0019 ± 0.0001
GRR	130 ± 20		0.0033 ± 0.003
SRR			0.0022 ± 0.0003
NB	63 ± 12		0.07 ± 0.01
NS	158 ± 3		0.022 ± 0.002
SP1	86 ± 4		0.035 ± 0.004
SP2	322 ± 15		0.0021 ± 0.0001
SPmix			0.0029 ± 0.0001
SNS	133 ± 12		0.0028 ± 0.0003
NBS			0.0063 ± 0.0008
DRR			0.0026 ± 0.0002
eRR	36 ± 5		0.032 ± 0.001
PEST			0.0054 ± 0.0003
Su9			0.099 ± 0.008
No tail			0.0015 ± 0.0002

tured human HEK293 cells. To ensure proteasome targeting, we used the Ubl domain of *S. pombe* Rhp23 (58) for the *S. pombe* experiments and the Ubl domain of human HR23B (59) for the HEK293 experiments, as well as appropriate vectors, promoters, and red fluorescent proteins (Fig. 6A). The steady-state levels of the Ubl-YFP-tail proteins, as assayed by YFP/RFP values, in the different organisms were highly correlated (Fig. 6, B–D). We conclude that the proteasomes of *S. cerevisiae*, *S. pombe*, and *Homo sapiens* share similar preferences for the amino acid sequence of their initiation sites.

Initiation Sequence Preferences Reflect Proteasome Affinity—Degradation rates of Ubl-YFP-tail proteins in *S. cerevisiae* correlated with degradation rates measured *in vitro* for a set of proteins with the same tails as tested here (Fig. 7A). In the *in vitro* experiments, the tails were attached to a DHFR domain that was targeted to the proteasome by a tetra-ubiquitin chain, and these Ub₄-DHFR-tail proteins were then degraded by purified *S. cerevisiae* proteasome (28).

To test whether initiation sequence preferences reflect a direct interaction with the proteasome, we developed an assay in which the different initiation regions compete with a substrate for degradation by purified *S. cerevisiae* proteasome. The substrate consisted of superfolder GFP with the Ubl domain from *S. cerevisiae* Rad23 fused to its N terminus and a disordered region of 95 amino acids derived from *S. cerevisiae* cytochrome *b*₂ fused to its C terminus. Degradation of this substrate by the proteasome in the presence of ATP, as assayed by loss of GFP fluorescence, followed Michaelis-Menten kinetics, with the V_{max} scaling linearly with proteasome concentration and the K_m remaining constant (Fig. 7B). We fused the different disordered tails described above to the C terminus of *E. coli* DHFR and purified the proteins from *E. coli* by affinity chromatography. We first characterized DHFR-35 and DHFR-eRR (where eRR is derived from *E. coli* lacI) (see supplemental Table S1 for sequences; 35, A; eRR, N). Both tails supported robust degradation of Ubl-YFP proteins in the cell (Figs. 2, 4–6). Increasing the concentrations of the DHFR-tail proteins progressively inhibited degradation of Ubl-GFP-95 (Fig. 7, C and

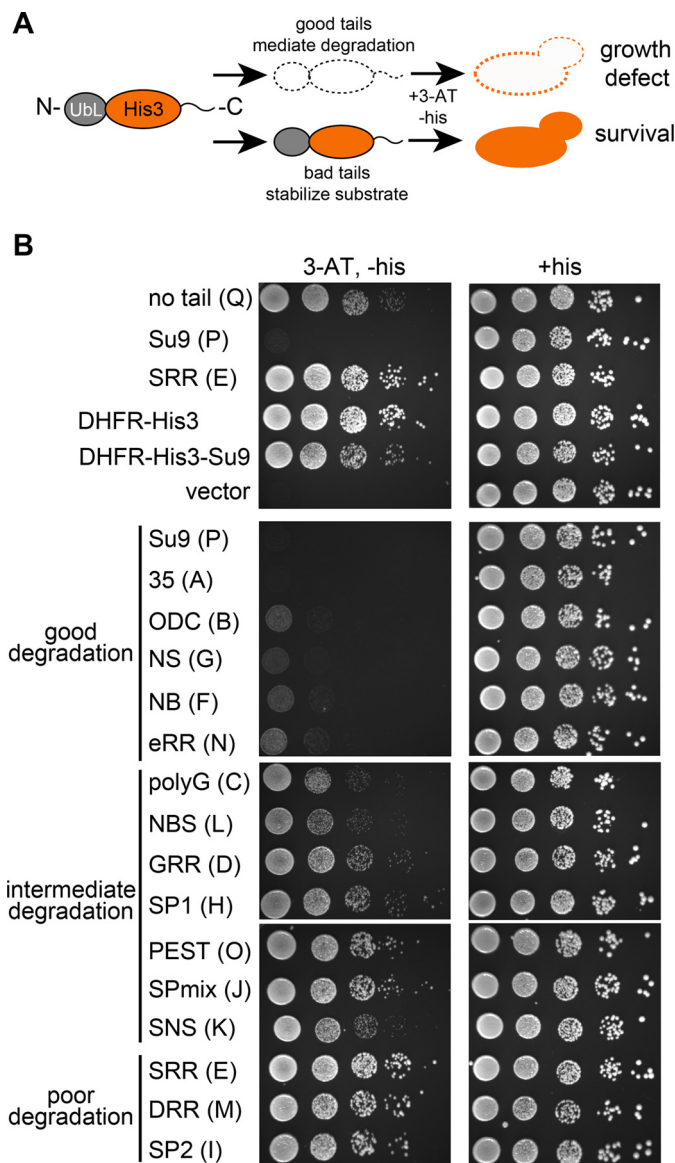


FIGURE 5. Analysis of proteasome initiation using His3 protein degradation in yeast. A, outline of the yeast growth assay. Imidazoleglycerol-phosphate dehydratase (His3) was targeted to the proteasome by fusing the Ubl domain of *S. cerevisiae* Rad23 to its N terminus and different tails to its C terminus. Only tails that provide effective proteasome initiation regions mediate His3 protein degradation. In *his3* mutant cells, the absence of His3 protein causes growth defects in medium lacking histidine. B, cells expressing the indicated His3 fusion proteins in late log phase were serially diluted and stamped onto selective (+3-AT, -his) or non-selective (+his) synthetic medium. Plates were incubated at 30 °C for 3 days before imaging.

D). Inhibition was overcome by increasing the Ubl-GFP-95 concentration, suggesting that Ubl-GFP-95 and the DHFR-tail proteins compete for binding to the proteasome's receptor for the initiation region (Fig. 7D). The apparent inhibition constants (K_i), with which the DHFR-tail proteins inhibited Ubl-GFP-95 degradation, therefore reflected the affinity of the tails for the proteasome.

We then selected a subset of initiation regions and measured their ability to inhibit Ubl-GFP-95 degradation (Table 2). The K_i values ranged from $\sim 30 \mu\text{M}$ for the highest affinity interaction to $\sim 300 \mu\text{M}$ for the weakest interaction. The inhibition constants for different tails correlated well ($R^2 = 0.73$) with

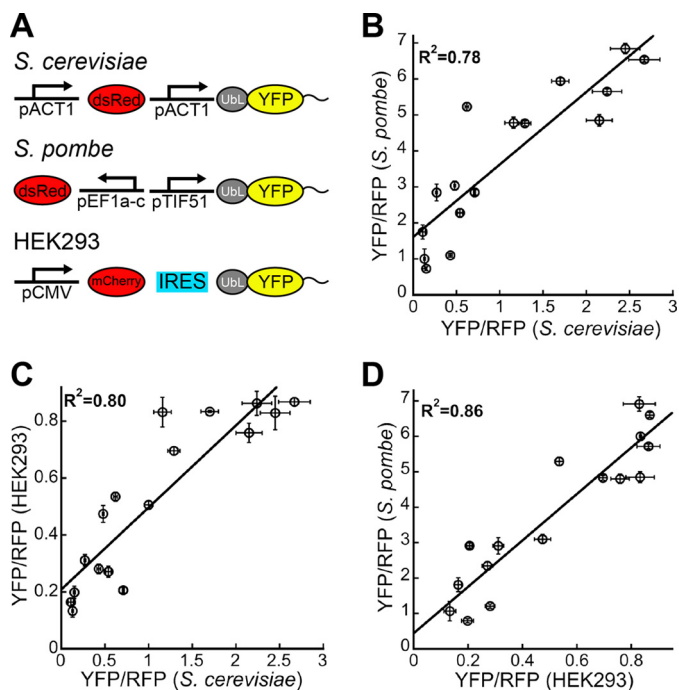


FIGURE 6. Conserved sequence preferences in different species. *A*, schematic representation of constructs used to assess proteasome targeting in *S. cerevisiae*, *S. pombe*, and cultured human cells (HEK293). In *S. cerevisiae*, YFP substrates and dsRed were both expressed from constitutive *act1* promoters on a CEN plasmid. In *S. pombe*, YFP substrates and dsRed were expressed from the constitutive promoters *tif51* and *ef1a-c*, respectively, after integration into genomic DNA. In HEK293 cells, mCherry and the YFP substrates were expressed from a single CMV promoter with their coding sequences separated by an internal ribosome entry site (*IRES*) on the mammalian expression vector pCDNA5. *B–D*, graphs plot corrected median cellular YFP fluorescence (median YFP/RFP values) for each construct expressed in two organisms against each other: *S. cerevisiae* and *S. pombe* (*B*), *S. cerevisiae* and HEK293 cells (*C*), and *S. pombe* and HEK293 cells (*D*). Correlation coefficients are calculated for fits to a straight line. The median YFP/RFP ratio for each construct was calculated from 10,000 cells collected in one flow cytometry run. Data points represent mean values determined from at least three repeat experiments; error bars indicate S.E.

their ability to support degradation, with tighter-binding tails leading to lower protein abundance in cells (Fig. 7E). Thus, the ability of disordered tails to initiate proteasomal degradation appears to be determined by their affinity for the proteasome.

Sequence Features of Initiation Regions—Which sequence characteristics of disordered tails dictate the proteasome's initiation preferences? To study initiation preferences in greater detail, we used the 16 sequences characterized above (supplemental Table S1) as well as 99 additional sequences derived primarily from human and yeast proteins, and we tested their effects on steady-state levels of UbL-YFP-tail proteins *in vivo* (supplemental Table S2). We calculated a set of parameters of these sequences that report on their chemical or physical properties, such as hydrophobicity, charge, sequence complexity, flexibility, etc. (Fig. 8A). The sequence characteristics of the complete set of 115 sequences tested represent the properties of the human proteome well (Fig. 8B).

The scales for which the parameters reporting sequence properties are assessed were not developed with protein degradation in mind, and there is no *a priori* reason to assume a linear relationship between these parameters and degradation rates. Therefore, we took a nonparametric approach when relating

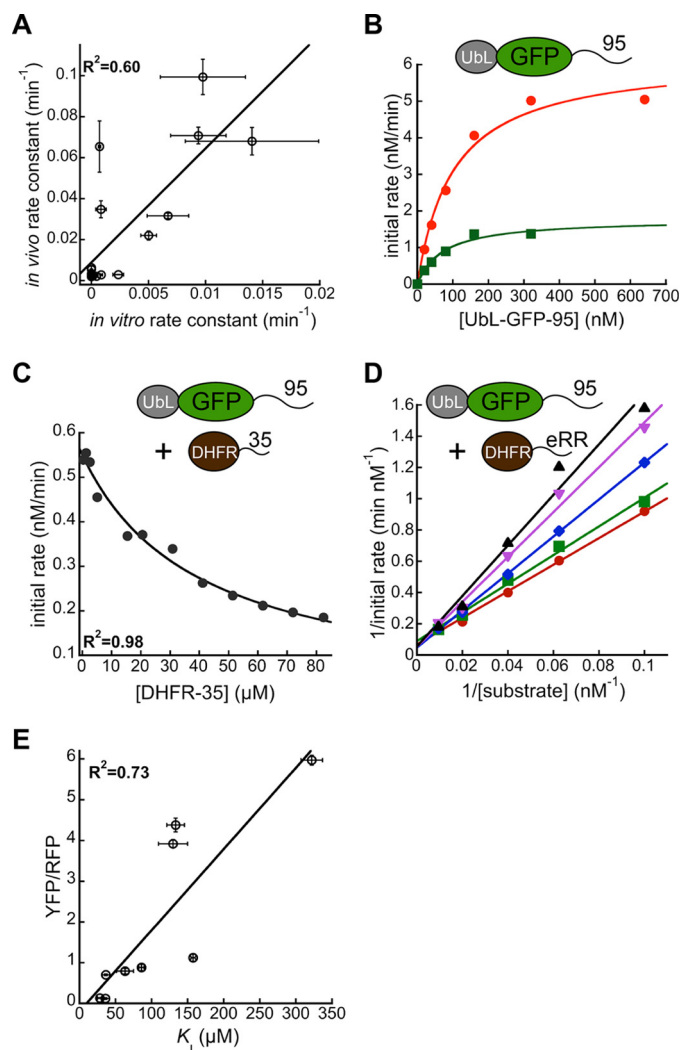


FIGURE 7. Binding of initiation sequences to the proteasome. *A*, correlation between substrate degradation rate constants *in vitro* and *in vivo*. Degradation rate constants *in vivo* for UbL-YFP-tail constructs as quoted in Table 2 are plotted against rate constants for degradation of Ub₄-DHFR-tail substrates by purified yeast proteasome (adopted from Ref. 28). The correlation coefficient is calculated for a fit to a straight line. *B*, Michaelis-Menten plot for UbL-GFP-95 degradation by 10 nM (green) or 40 nM (red) purified *S. cerevisiae* proteasome. The substrate consisted of an N-terminal UbL domain derived from *S. cerevisiae* Rad23, followed by superfolder GFP and a 95-amino acid-long tail derived from *S. cerevisiae* cytochrome *b*₂. *C*, initial degradation rates of UbL-GFP-95 in the presence of different concentrations of purified DHFR-35 by purified yeast proteasome are plotted and fitted to an equation describing competitive inhibition to calculate the inhibition constant K_i for DHFR-35. *D*, initial degradation rates for different concentrations of UbL-GFP-95 in the presence of 0 μ M (red), 2.6 μ M (green), 10 μ M (blue), 31 μ M (pink), or 95 μ M (black) DHFR-eRR. *E*, corrected median cellular YFP fluorescence (median YFP/RFP values) for cultures expressing fluorescent proteasome substrates with different tails at their C termini (pPGK1 dsRed, pTPI1 UbL-YFP-tail; Table 1) are plotted against the K_i values for DHFR-tail constructs with the same tail (Table 2). The correlation coefficient is calculated for a fit to a straight line. UbL-GFP-95 degradation was followed by monitoring fluorescence intensity over time using a Tecan plate reader at room temperature as described under the "Experimental Procedures." Tail sequences are shown in supplemental Table S1 (35, A; eRR, N).

the sequence parameters to protein degradation, using Spearman correlation coefficients to compare only the rank ordering of the different sequences by the various parameters with the rank ordering by YFP/RFP ratios. The correlations were tested for statistical significance (no correlation is the null hypothe-

Sequence Preferences in Proteasome Degradation

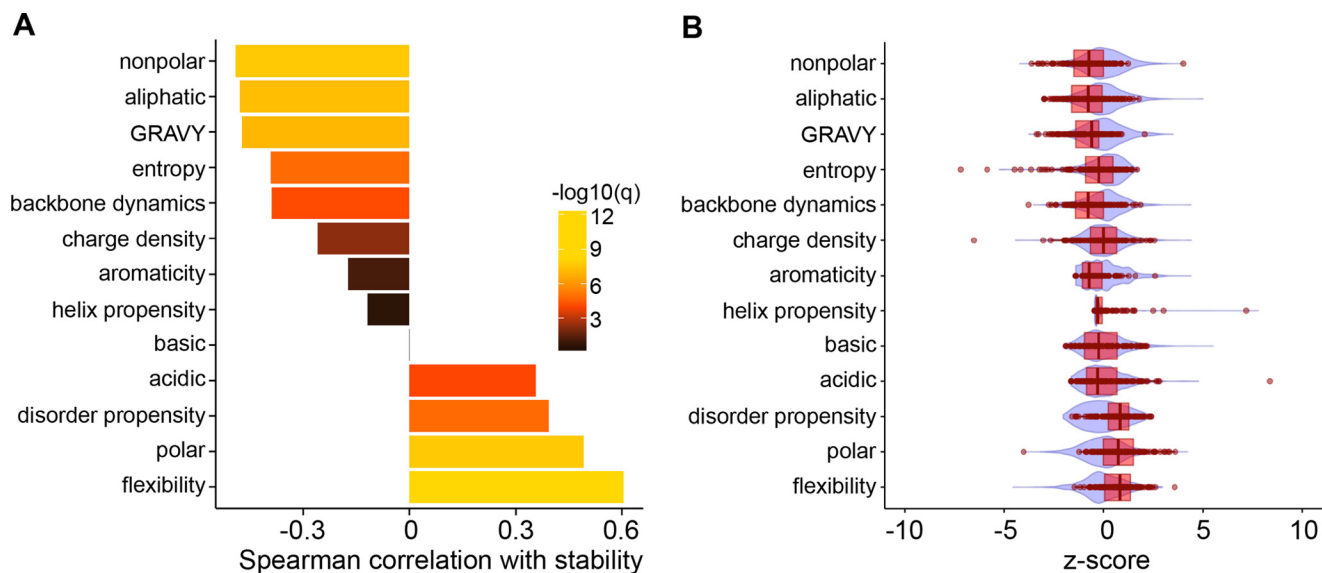


FIGURE 8. Bioinformatics analysis of initiation sequences. *A*, Spearman correlations between experimentally determined stabilities (measured by steady-state YFP/RFP ratios in Table 1 and supplemental Table S2 (pPGK1 dsRed, pTPI1 UbL-YFP-tail)) and physicochemical parameters of peptide sequences. The parameters for 115 sequences were calculated as described under the “Experimental Procedures.” Spearman correlation coefficients between the physicochemical parameters of the different sequences and YFP/RFP ratios were calculated. Statistical significance of these associations was accessed by pairwise *t* tests. The *p* values from *t* tests were then used to compute false discovery rate *q*-values by the Benjamini-Hochberg method (60), which are indicated in color ($-\log_{10}(q)$). *B*, comparison of the distribution of the parameters calculated for the 115 sequences analyzed in this study (box plots in red) and the same values calculated for the human proteome (violin plot in blue). A designed polypeptide library that covers the human proteome (T7-pep) (104) was used to represent the sequence characteristics of human proteome. The parameters were calculated as described under the “Experimental Procedures.”

sis), with *p* values adjusted for false discovery by the Benjamini-Hochberg method (Fig. 8A) (60).

Consistent with our previous study (28), we found sequence complexity (measured as sequence entropy) to be correlated negatively with protein stability, suggesting that initiation sequences with biased amino acid compositions support proteasome initiation inefficiently (Fig. 8A). In addition to sequence complexity, hydrophobicity of the initiation region as measured by the fraction of aliphatic residues, the fraction of nonpolar residues, or the GRAVY algorithm (61) correlated negatively with stability (Fig. 8A). In contrast, sequence polarity (fraction of Asp, Glu, His, Lys, Asn, Arg, Ser, and Thr) and sequence acidity (fraction of Asp and Glu) correlated positively with stability (Fig. 8A). Thus, proteasome initiation seems more efficient at less hydrophilic and more hydrophobic regions.

Sequence dynamics also affect proteasome initiation and stiffer initiation regions appeared to promote better recognition and degradation. This relationship was found using two independent algorithms to predict sequence flexibility. The FLEXPLOT algorithm (62) predicts sequence flexibility by an algorithm calibrated using crystallographic B-factors, whereas the DynaMine tool predicts backbone dynamics through an algorithm calibrated by residue dynamics measured by nuclear magnetic resonance spectroscopy (63, 64). The two algorithms define their scales in opposite directions; the FLEXPLOT algorithm assigns numerically lower scores to stiffer sequences, and the DynaMine algorithm assigns numerically higher scores. Analysis based on the DynaMine algorithm resulted in a negative correlation between its score and stability, whereas the FLEXPLOT algorithm results in a positive correlation (Fig. 8A).

Discussion

We find that the proteasome has distinct preferences for the amino acid sequence where it initiates degradation *in vivo*. Initiation regions tune protein abundance over 2 orders of magnitude, which is the same range as achieved by controlling ubiquitination of a classical N-end rule degron. Proteasomal initiation may regulate protein abundance over an even larger range, but our experimental system is limited by the level of protein expression and by signal over noise detection. Therefore, the proteasome’s sequence preferences at the initiation step of degradation can contribute substantially to the regulation of protein abundance in the cell.

The ubiquitin code is ambiguous in that the proteasome can recognize polyubiquitin chains that typically target proteins to other processes. For example, polyubiquitin chains linked through Lys-63 are usually part of membrane trafficking processes, but they can target a protein to the proteasome both *in vitro* and *in vivo* (18). Proteins that are tagged with ubiquitin chains for fates other than degradation may have evolved to lack effective proteasome initiation sites to reduce the likelihood of degradation if they bind the proteasome. Conversely, if the proteasome is able to engage its target efficiently at the initiation region, even a weakly binding ubiquitin chain may induce degradation. Indeed, the presence of predicted proteasome initiation regions correlates with shorter protein half-lives *in vivo* (23, 27–29). Thus, natural variation in the unstructured regions of protein paralogs could tune protein abundance by modulating proteasomal initiation. Similarly, mechanisms that alter disordered regions such as alternative splicing (65, 66) could be used to tune protein abundance.

At the same time, the different polyubiquitin chains that target proteins to the proteasome physiologically are not necessarily synonymous. Cell cycle progression requires the degradation of regulatory proteins in the correct order. Some of these regulatory proteins are ubiquitinated by the same master ubiquitin ligase and ubiquitin-conjugating enzyme, but the polyubiquitin chains are synthesized with different efficiencies (67–69). The initiation step could contribute to substrate ordering if the late substrates, which are ubiquitinated less efficiently, also had less effective initiation regions and vice versa. Thus, the proteasome's initiation sequence preferences could contribute to the temporal control of degradation.

The proteasome's sequence preferences may also contribute to the accumulation of disease-related proteins. Several neurodegenerative diseases are associated with the buildup of proteins that appear to be targeted for degradation but escape destruction (70). Several of these proteins contain highly biased amino acid sequences. For example, the protein linked to Huntington disease (HTT exon1) is rich in proline and glutamine residues. It is in a disordered conformation but escapes proteasomal degradation even when ubiquitinated, apparently because of its biased sequence (28, 71, 72). Similar biased sequences also exist in the PRNP protein, which is associated with prion disease, in α -synuclein, which is associated with Parkinson disease and other disease-related proteins. The worst initiation regions analyzed here all share a biased amino acid composition with some amino acids strongly over-represented and others missing entirely (28). It is possible that the amino acid composition of the proteins associated with neurodegenerative diseases also makes them more difficult to be recognized by the proteasome and contributes to their accumulation in cells.

The proteasome's sequence preferences are conserved in *S. cerevisiae*, *S. pombe*, and cultured human cells, and they reflect a direct physical interaction between the initiation region in the substrate protein and the proteasome. The receptor of the initiation region on the proteasome is not known, but a likely site is the degradation channel that leads through the ATPase ring of the activator cap to the proteolytic chamber in the core of the proteasome.

The degradation channel is lined by two sets of loops, the P1 and P2 loops, and their sequences are conserved between eukaryotic proteasomes and bacterial AAA⁺ proteases, which fulfill similar functions as the proteasome (2, 73–79). The biochemical mechanism of the *E. coli* AAA⁺ protease ClpXP is particularly well understood (79). The P1 loops undergo conformational changes during ATP-dependent proteolysis and are thought to act as paddles that move the polypeptide chain through the pore (77, 78, 80–82) toward a second binding site formed by the P2 loops (80). Binding to the second site may prevent backsliding of the polypeptide chains between strokes of the P1 paddles (80).

By analyzing ~100 different initiation regions, we were able to determine some sequence properties that govern how well the proteasome is able to initiate degradation. For example, stiffer initiation regions lead to more rapid degradation, perhaps because they increase the distance through space that an initiation region can explore. The P1 loops are located 1–3 nm

from the entrance to the degradation channel as judged by the proteasome structure (83–86) so that stiffer sequences may be able to reach the P1 loops and engage the translocation motor more efficiently than more flexible sequences. The preference for hydrophobic initiation sequences may reflect their ability to interact with the P1 paddles, which have the consensus sequence aromatic-hydrophobic-Gly. The stabilizing effect of acidic sequences may be a reflection of weaker interaction between these sequences and the P2 loop region, which contains Glu and Asp in the proteasome. The sequence preferences could also be a reflection of consensus sequences in initiation regions that are recognized by their receptor on the proteasome. The relationship between sequence complexity and proteasome degradation could then be explained by the fact that biased sequences would be less likely to contain sequences that resemble the consensus motif than diverse sequences (28).

Bacterial AAA⁺ proteases can recognize their substrates and initiate degradation at the same sequences. These targeting sequences fulfill both the recognition and initiation functions, although recognition can be enhanced by targeting adaptors (87). Some 20 ClpXP degrons have been described in *E. coli* (88). The degrons are 10–12 amino acids long (88) and thus appear to be shorter than the proteasome initiation regions discussed here. The shorter length is consistent with the fact that the P1 loops in ClpX are also closer to the entrance to the degradation channel than in the proteasome. One of the bacterial targeting sequences, the SsrA tag, is particularly well characterized and binds ClpXP with ~1 μ M affinity (79). The sequence of the SsrA degron is precisely defined in the sense that single amino acid substitutions can reduce degradation drastically (88). Some eukaryotic proteins are targeted to the proteasome in the absence of ubiquitin, with ODC as the best characterized example (89). However, even the ODC initiation region binds the proteasome with considerably lower affinity than the SsrA tag. Efficient ODC degradation requires the protein Antizyme to serve as an adaptor that increases ODC's affinity to the proteasome (90, 91) in analogy to the bacterial adaptor proteins. So far the proteasome initiation regions seem to be less precisely defined than the ClpXP degrons (88), and the results summarized here did not reveal specific consensus motifs that are recognized by the proteasome. Larger sequence libraries will have to be analyzed to reveal such consensus sequences, if they exist.

In summary, we show that *in vivo* the proteasome has pronounced preferences for the amino acid sequence of its targets at the site where it initiates degradation. The selection of initiation sites represents a degradation code that is embedded within the target proteins. This initiation code is as important and operates in parallel to the ubiquitin code. Its evolutionary conservation suggests that the mechanism may alter the abundance distribution of the proteome in a wide variety of cells and organisms, affecting diverse genetic and regulatory processes.

Experimental Procedures

Substrate Proteins—Proteasome substrate proteins were derived from *E. coli* DHFR, *S. cerevisiae* His3, superfolder GFP (53), and a rapidly maturing derivative of YFP (a gift from B. S. Glick (University of Chicago)). N-terminal UbL domains from

Sequence Preferences in Proteasome Degradation

S. cerevisiae Rad23 or its homologs in *S. pombe* (Rhp23) and human cells (human HR23B) were connected to His3, GFP, or YFP by the linker sequence (VDGGSSGGGS). C-terminal tails were attached through a 2-amino acid linker (Pro-Arg), and the amino acid sequences of the tails are shown in supplemental Tables S1 and S2.

Protein Expression and Purification—Yeast proteasome was purified from *S. cerevisiae* strain YYS40 by immunoaffinity chromatography using FLAG antibodies (M2-agarose affinity beads, Sigma), as described previously (92). Proteasome preparations were analyzed by SDS-PAGE and compared with published compositions (83). Each proteasome preparation was tested for activity by measuring degradation of the proteasome substrate UbL-DHFR-95 and for contamination by proteases by testing for stability of proteins that lack a proteasome-binding tag (DHFR-95) as described previously (57, 93).

The substrate (UbL-GFP-95) and competitor proteins (His₁₀-DHFR-tail) used in *in vitro* inhibition assays were overexpressed in *E. coli* and purified using standard methods. Constructs were cloned into a pET3a vector and expressed from the T7 promoter in *E. coli* strains BL21(DE3)pLysS or Rosetta(DE3)pLysS (Novagen). Proteins were purified by TALON metal affinity beads (catalog no. 635502, Clontech) following the manufacturer's instructions. Purified proteins were dialyzed into buffer containing 50 mM Tris, pH 7.4, 300 mM NaCl, and 1% glycerol for storage. Protein concentrations were determined by measuring light absorbance at 280 nm and using extinction coefficients predicted from the proteins' sequence (ExpASY's ProtParam). The integrity and purity of proteins were evaluated by SDS-PAGE.

Competition Assays—The degradation of a fluorescent substrate protein (UbL-GFP-95) *in vitro* was monitored by measuring GFP fluorescence intensity over time in 384-well plates using a plate reader (Infinite M1000 PRO, Tecan) as described previously (94). Assays were carried out at 30 °C by adding fluorescent substrates at the indicated concentrations to 40 nM purified yeast proteasome in a reaction buffer (50 mM Tris, 5 mM MgCl₂, 2.5% glycerol, 1 mM ATP, 4 mM DTT, 0.2 mg ml⁻¹ bovine serum albumin, 10 mM creatine phosphate, 0.1 mg ml⁻¹ creatine kinase, pH 7.5). Fluorescence intensity was read every 30 s for 1 h (excitation, 485 nm/5 nm bandwidth; emission, 535 nm/10 nm bandwidth). Protein amounts were confirmed by comparing the fluorescence intensity of the reaction in each well with calibration curves relating fluorescence intensity to protein concentration. Each assay was repeated at least three times. Initial degradation rates representing the slope of the decay curves at time 0 were calculated as the product of the amplitude, and the rate constant was determined by nonlinear fitting of the time-dependent fluorescence change to the equation describing single exponential decay to a constant offset using the software package KaleidaGraph (version 4.1, Synergy Software).

Yeast Expression—In *S. cerevisiae*, fluorescent proteins were expressed from a CEN plasmid (YCplac33) and His3 proteins from a 2-micron plasmid (pYES2), both with a URA3 selection marker. The plasmids were transformed into *S. cerevisiae* strain BY4741, which carries a deletion of the efflux pump Pdr5 (see

supplemental Table S3 for genotype) (95) using Frozen-EZ Yeast Transformation II kit (Zymo Research).

In *S. pombe*, fluorescent proteins were expressed after integration into the genome using pDUAL-derived plasmids (96). 2 μg of plasmid were digested with NotI and purified (Qiagen). Frozen competent cells of *S. pombe* (see supplemental Table S3 for genotype) were thawed in a 30 °C water bath for 2 min, mixed with purified plasmid DNA, and 30% PEG 3350. The mixture was vortexed, incubated at 30 °C for 1 h, heat shocked at 43 °C for 15 min, and placed at room temperature for 10 min. The cells were then pelleted at 1600 × *g* for 3 min and resuspended in 500 μl of ½YE (0.25% yeast extract, 1.5% glucose). Cells were shaken for 1 h at 30 °C and spread onto synthetic medium lacking leucine. Clones with a single cassette integrated were validated by PCR.

The proteasome substrates and the RFP dsRed-Express2 (38) were expressed from separate promoters on the *S. cerevisiae* and *S. pombe* plasmids as specified. Proteasome activity was inhibited by 100 μM bortezomib. Protein synthesis was inhibited by 125 μM cycloheximide. 2% glucose was used to turn off protein expression from the promoter *gal1*.

Cell Culture Expression—Fluorescent proteins were expressed from the vector pCDNA5 (Life Technologies, Inc.) transiently transfected into HEK293 cells. The proteasome substrates and the RFP mCherry (97) were expressed from a single CMV promoter with the coding regions separated by an internal ribosome entry site derived from encephalomyocarditis virus (98).

HEK293 cells were cultured at 37 °C and 5% CO₂ in DMEM supplemented with 10% FBS, 100 units/ml penicillin, and 100 units/ml streptomycin (Life Technologies, Inc.). Cells were seeded in a 6-well plate at 0.5 × 10⁶ cells/ml 24 h prior to transfection. 1 μg of DNA was transfected into cells with Lipofectamine 2000 (Life Technologies, Inc.) for 24 h. Cells were washed with PBS and recovered in complete DMEM for 24 h before analysis.

Yeast Growth Assay—His3 proteins were expressed from the inducible *gal1* promoter on a 2-micron plasmid (pYES2) with a URA3 selection marker in *S. cerevisiae* strain *pdr5Δ* (see supplemental Table S3 for genotype). Cells were grown with galactose as the carbon source at 30 °C to late log phase, serially diluted (*A*₆₀₀ from 10⁻¹ to 10⁻⁶) and stamped on plates with synthetic defined drop-out medium. Where indicated, 10 mM 3-AT was added to the medium as a competitive inhibitor of His3 to enhance assay sensitivity (55). Plates were incubated at 30 °C for 3 days for imaging.

Flow Cytometry—Yeast cells were grown at 30 °C to early log phase. HEK293 cells were grown for 24 h after transfection, trypsinized with TrypLE (Life Technologies, Inc.), washed, suspended in 0.5 ml of phosphate-buffered saline (PBS), and fixed by the addition of 0.5 ml of 3.7% formaldehyde in PBS. The fluorescence signals in the dsRed (or mCherry) and YFP (or GFP) channels were measured in a flow cytometer (LSR Fortessa, BD Biosciences) and analyzed by FlowJo software to calculate the medians of the YFP over RFP fluorescence ratios for each population. Each assay was repeated at least three times.

Western Blot—Yeast cells were grown to mid-log phase and lysed by vortexing with glass beads (BioSpec Products). Protein extracts were prepared and analyzed by Western blotting using standard protocols as described (28). YFP fusion proteins were detected with a mouse monoclonal anti-enhanced GFP antibody (1:1000, Clontech, catalog no. 632569) and an Alexa-800-labeled goat anti-mouse secondary antibody (1:20,000, Rockland Immunochemicals, catalog no. 610-132-121). Scs2 was detected by an anti-Scs2 rabbit polyclonal antibody (28) (1:1000, gift from J. Brickner, Northwestern University) and an Alexa-680 goat anti-rabbit secondary antibody (1:20,000, Invitrogen, catalog no. A21109). Protein amounts were estimated by direct infrared fluorescence imaging (Odyssey LI-COR Biosciences).

Bioinformatics and Statistical Analysis—The physicochemical properties of 115 sequences were calculated using the following tools: helix propensity, Agadir (99); backbone dynamics, DynaMine (63, 64); disorder propensity, IUPred (100); fraction of aliphatic, acidic, basic, nonpolar, aromatic or polar residues: EMBOSS pepstats (101); entropy, SEG (102, 103); flexibility, FLEXPLOT (62); and hydrophobicity, GRAVY (61). The charge density was calculated as the fraction of basic amino acids minus the fraction of acidic amino acids. Note that the flexibility prediction method of Vihenen *et al.* (62) was optimized for short windows of nine amino acid residues, although we calculated an aggregate flexibility score (mean flex (62)) by averaging the flexibility values for all consecutive nine-residue windows. To avoid making assumptions about the relationships between degradation rates and the numerical values of the sequence properties on their varied scales, we quantified the association of each metric with protein stability using the nonparametric Spearman rank correlation coefficients. Statistical significance of these associations was assessed by testing the hypothesis that a particular parameter does not correlate with degradation using pairwise *t* tests. The *p* values resulting from these tests were then used to compute false discovery rate *q*-values using the Benjamini-Hochberg method (60).

Author Contributions—H. Y., A. K. S. G., S. R. W., D. W., G. K., K. M., M. W., S. C., and T. I. performed the experiments, analyzed the data, and co-wrote the paper. I. J. F., M. M. B., and A. M. directed the experiments, analyzed the data, and co-wrote the paper.

Acknowledgments—We thank Drs. Ben S. Glick (University of Chicago), Jason Brickner (Northwestern University), Raymond Deshaies (California Institute of Technology), Robert T. Sauer (Massachusetts Institute of Technology), Akihisa Matsuyama (RIKEN), as well as Christopher M. Yellman, Blerta Xhemalce, and Richard Salinas (The University of Texas at Austin) for advice and reagents. We are grateful to Kimberly Bowen and Rachael Rossi for constructing *S. pombe* strains. We acknowledge the use of the instruments of the Microscopy and Imaging Facility of the Institute for Cell and Molecular Biology at The University of Texas at Austin.

References

1. Finley, D. (2009) Recognition and processing of ubiquitin-protein conjugates by the proteasome. *Annu. Rev. Biochem.* **78**, 477–513
2. Finley, D., Chen, X., and Walters, K. J. (2016) Gates, channels, and switches: elements of the proteasome machine. *Trends Biochem. Sci.* **41**, 77–93
3. Komander, D., and Rape, M. (2012) The ubiquitin code. *Annu. Rev. Biochem.* **81**, 203–229
4. Husnjak, K., and Dikic, I. (2012) Ubiquitin-binding proteins: decoders of ubiquitin-mediated cellular functions. *Annu. Rev. Biochem.* **81**, 291–322
5. Thrower, J. S., Hoffman, L., Rechsteiner, M., and Pickart, C. M. (2000) Recognition of the polyubiquitin proteolytic signal. *EMBO J.* **19**, 94–102
6. Terrell, J., Shih, S., Dunn, R., and Hicke, L. (1998) A function for monoubiquitination in the internalization of a G protein-coupled receptor. *Mol. Cell* **1**, 193–202
7. Hicke, L., and Riezman, H. (1996) Ubiquitination of a yeast plasma membrane receptor signals its ligand-stimulated endocytosis. *Cell* **84**, 277–287
8. Galan, J. M., and Haguenuer-Tsapis, R. (1997) Ubiquitin lys63 is involved in ubiquitination of a yeast plasma membrane protein. *EMBO J.* **16**, 5847–5854
9. Jackson, S. P., and Durocher, D. (2013) Regulation of DNA damage responses by ubiquitin and SUMO. *Mol. Cell* **49**, 795–807
10. Kirkpatrick, D. S., Hathaway, N. A., Hanna, J., Elsasser, S., Rush, J., Finley, D., King, R. W., and Gygi, S. P. (2006) Quantitative analysis of *in vitro* ubiquitinated cyclin B1 reveals complex chain topology. *Nat. Cell Biol.* **8**, 700–710
11. Xu, P., Duong, D. M., Seyfried, N. T., Cheng, D., Xie, Y., Robert, J., Rush, J., Hochstrasser, M., Finley, D., and Peng, J. (2009) Quantitative proteomics reveals the function of unconventional ubiquitin chains in proteasomal degradation. *Cell* **137**, 133–145
12. Dimova, N. V., Hathaway, N. A., Lee, B.-H., Kirkpatrick, D. S., Berkowitz, M. L., Gygi, S. P., Finley, D., and King, R. W. (2012) APC/C-mediated multiple monoubiquitylation provides an alternative degradation signal for cyclin B1. *Nat. Cell Biol.* **14**, 168–176
13. Kravtsova-Ivantsiv, Y., Cohen, S., and Ciechanover, A. (2009) Modification by single ubiquitin moieties rather than polyubiquitination is sufficient for proteasomal processing of the p105 NF- κ B precursor. *Mol. Cell* **33**, 496–504
14. Lu, Y., Lee, B.-H., King, R. W., Finley, D., and Kirschner, M. W. (2015) Substrate degradation by the proteasome: a single-molecule kinetic analysis. *Science* **348**, 1250834–1250834
15. Shabek, N., Herman-Bachinsky, Y., and Ciechanover, A. (2009) Ubiquitin degradation with its substrate, or as a monomer in a ubiquitination-independent mode, provides clues to proteasome regulation. *Proc. Natl. Acad. Sci. U.S.A.* **106**, 11907–11912
16. Baboshina, O. V., and Haas, A. L. (1996) Novel multiubiquitin chain linkages catalyzed by the conjugating enzymes E2EPF and RAD6 are recognized by 26 S proteasome subunit 5. *J. Biol. Chem.* **271**, 2823–2831
17. Hofmann, R. M., and Pickart, C. M. (2001) *In vitro* assembly and recognition of Lys-63 polyubiquitin chains. *J. Biol. Chem.* **276**, 27936–27943
18. Saeki, Y., Kudo, T., Sone, T., Kikuchi, Y., Yokosawa, H., Toh-e, A., and Tanaka, K. (2009) Lysine 63-linked polyubiquitin chain may serve as a targeting signal for the 26S proteasome. *EMBO J.* **28**, 359–371
19. Nathan, J. A., Kim, H. T., Ting, L., Gygi, S. P., and Goldberg, A. L. (2013) Why do cellular proteins linked to K63-polyubiquitin chains not associate with proteasomes? *EMBO J.* **32**, 552–565
20. Jacobson, A. D., Zhang, N.-Y., Xu, P., Han, K.-J., Noone, S., Peng, J., and Liu, C.-W. (2009) The lysine 48 and lysine 63 ubiquitin conjugates are processed differently by the 26 S proteasome. *J. Biol. Chem.* **284**, 35485–35494
21. Prakash, S., Tian, L., Ratliff, K. S., Lehoczky, R. E., and Matouschek, A. (2004) An unstructured initiation site is required for efficient proteasome-mediated degradation. *Nat. Struct. Mol. Biol.* **11**, 830–837
22. Takeuchi, J., Chen, H., and Coffino, P. (2007) Proteasome substrate degradation requires association plus extended peptide. *EMBO J.* **26**, 123–131
23. van der Lee, R., Lang, B., Kruse, K., Gsponer, J., Sánchez de Groot, N., Huynen, M. A., Matouschek, A., Fuxreiter, M., and Babu, M. M. (2014) Intrinsically disordered segments affect protein half-life in the cell and during evolution. *Cell Rep.* **8**, 1832–1844
24. Zhao, M., Zhang, N.-Y., Zurawel, A., Hansen, K. C., and Liu, C.-W. (2010) Degradation of some polyubiquitinated proteins requires an intrinsic proteasomal binding element in the substrates. *J. Biol. Chem.* **285**, 4771–4780

25. Prakash, S., Inobe, T., Hatch, A. J., and Matouschek, A. (2009) Substrate selection by the proteasome during degradation of protein complexes. *Nat. Chem. Biol.* **5**, 29–36
26. Inobe, T., Fishbain, S., Prakash, S., and Matouschek, A. (2011) Defining the geometry of the two-component proteasome degron. *Nat. Chem. Biol.* **7**, 161–167
27. Fishbain, S., Prakash, S., Herrig, A., Elsasser, S., and Matouschek, A. (2011) Rad23 escapes degradation because it lacks a proteasome initiation region. *Nat. Commun.* **2**, 192
28. Fishbain, S., Inobe, T., Israeli, E., Chavali, S., Yu, H., Kago, G., Babu, M. M., and Matouschek, A. (2015) Sequence composition of disordered regions fine-tunes protein half-life. *Nat. Struct. Mol. Biol.* **22**, 214–221
29. Guharoy, M., Bhowmick, P., Sallam, M., and Tompa, P. (2016) Tripartite degrons confer diversity and specificity on regulated protein degradation in the ubiquitin-proteasome system. *Nat. Commun.* **7**, 10239
30. Rape, M., Hoppe, T., Gorr, I., Kalocay, M., Richly, H., and Jentsch, S. (2001) Mobilization of processed, membrane-tethered SPT23 transcription factor by CDC48(UFD1/NPL4), a ubiquitin-selective chaperone. *Cell* **107**, 667–677
31. Richly, H., Rape, M., Braun, S., Rumpf, S., Hoege, C., and Jentsch, S. (2005) A series of ubiquitin binding factors connects CDC48/p97 to substrate multiubiquitylation and proteasomal targeting. *Cell* **120**, 73–84
32. Wójcik, C., Rowicka, M., Kudlicki, A., Nowis, D., McConnell, E., Kujawa, M., and DeMartino, G. N. (2006) Valosin-containing protein (p97) is a regulator of endoplasmic reticulum stress and of the degradation of N-end rule and ubiquitin-fusion degradation pathway substrates in mammalian cells. *Mol. Biol. Cell* **17**, 4606–4618
33. Beskow, A., Grimberg, K. B., Bott, L. C., Salomons, F. A., Dantuma, N. P., and Young, P. (2009) A conserved unfoldase activity for the p97 AAA-ATPase in proteasomal degradation. *J. Mol. Biol.* **394**, 732–746
34. Raman, M., Havens, C. G., Walter, J. C., and Harper, J. W. (2011) A genome-wide screen identifies p97 as an essential regulator of DNA damage-dependent CDT1 destruction. *Mol. Cell* **44**, 72–84
35. Verma, R., Oania, R., Fang, R., Smith, G. T., and Deshaies, R. J. (2011) Cdc48/p97 mediates UV-dependent turnover of RNA Pol II. *Mol. Cell* **41**, 82–92
36. Barthelme, D., and Sauer, R. T. (2012) Identification of the Cdc48-20S proteasome as an ancient AAA⁺ proteolytic machine. *Science* **337**, 843–846
37. Partow, S., Siewers, V., Bjørn, S., Nielsen, J., and Maury, J. (2010) Characterization of different promoters for designing a new expression vector in *Saccharomyces cerevisiae*. *Yeast* **27**, 955–964
38. Strack, R. L., Strongin, D. E., Bhattacharyya, D., Tao, W., Berman, A., Broxmeyer, H. E., Keenan, R. J., and Glick, B. S. (2008) A noncytotoxic DsRed variant for whole-cell labeling. *Nat. Methods* **5**, 955–957
39. Sharon, E., Kalma, Y., Sharp, A., Raveh-Sadka, T., Levo, M., Zeevi, D., Keren, L., Yakhini, Z., Weinberger, A., and Segal, E. (2012) Inferring gene regulatory logic from high-throughput measurements of thousands of systematically designed promoters. *Nat. Biotechnol.* **30**, 521–530
40. Yen, H.-C., Xu, Q., Chou, D. M., Zhao, Z., and Elledge, S. J. (2008) Global protein stability profiling in mammalian cells. *Science* **322**, 918–923
41. Elsasser, S., Gali, R. R., Schwickart, M., Larsen, C. N., Leggett, D. S., Müller, B., Feng, M. T., Tübing, F., Dittmar, G. A., and Finley, D. (2002) Proteasome subunit Rpn1 binds ubiquitin-like protein domains. *Nat. Cell Biol.* **4**, 725–730
42. Husnjak, K., Elsasser, S., Zhang, N., Chen, X., Randles, L., Shi, Y., Hofmann, K., Walters, K. J., Finley, D., and Dikic, I. (2008) Proteasome subunit Rpn13 is a novel ubiquitin receptor. *Nature* **453**, 481–488
43. Shi, Y., Chen, X., Elsasser, S., Stocks, B. B., Tian, G., Lee, B.-H., Shi, Y., Zhang, N., de Poot, S. A., Tübing, F., Sun, S., Vannoy, J., Tarasov, S. G., Engen, J. R., Finley, D., and Walters, K. J. (2016) Rpn1 provides adjacent receptor sites for substrate binding and deubiquitination by the proteasome. *Science* **351**, aad9421
44. Collins, G. A., Gomez, T. A., Deshaies, R. J., and Tansey, W. P. (2010) Combined chemical and genetic approach to inhibit proteolysis by the proteasome. *Yeast* **27**, 965–974
45. Crawford, L. J., Walker, B., Ovaa, H., Chauhan, D., Anderson, K. C., Morris, T. C., and Irvine, A. E. (2006) Comparative selectivity and specificity of the proteasome inhibitors BzLLCCHO, PS-341, and MG-132. *Cancer Res.* **66**, 6379–6386
46. McGrath, J. P., Jentsch, S., and Varshavsky, A. (1991) UBA 1: an essential yeast gene encoding ubiquitin-activating enzyme. *EMBO J.* **10**, 227–236
47. Ghaboosi, N., and Deshaies, R. J. (2007) A conditional yeast E1 mutant blocks the ubiquitin-proteasome pathway and reveals a role for ubiquitin conjugates in targeting Rad23 to the proteasome. *Mol. Biol. Cell* **18**, 1953–1963
48. Bercovich, Z., Rosenberg-Hasson, Y., Ciechanover, A., and Kahana, C. (1989) Degradation of ornithine decarboxylase in reticulocyte lysate is ATP-dependent but ubiquitin-independent. *J. Biol. Chem.* **264**, 15949–15952
49. Murakami, Y., Matsufuji, S., Kameji, T., Hayashi, S., Igarashi, K., Tamura, T., Tanaka, K., and Ichihara, A. (1992) Ornithine decarboxylase is degraded by the 26S proteasome without ubiquitination. *Nature* **360**, 597–599
50. Strack, R. L., Keenan, R. J., and Glick, B. S. (2011) Noncytotoxic DsRed derivatives for whole-cell labeling. *Methods Mol. Biol.* **699**, 355–370
51. Bachmair, A., Finley, D., and Varshavsky, A. (1986) *In vivo* half-life of a protein is a function of its amino-terminal residue. *Science* **234**, 179–186
52. Bachmair, A., and Varshavsky, A. (1989) The degradation signal in a short-lived protein. *Cell* **56**, 1019–1032
53. Pédelacq, J.-D., Cabantous, S., Tran, T., Terwilliger, T. C., and Waldo, G. S. (2006) Engineering and characterization of a superfolder green fluorescent protein. *Nat. Biotechnol.* **24**, 79–88
54. Alifano, P., Fani, R., Liò, P., Lazcano, A., Bazzicalupo, M., Carlomagno, M. S., and Bruni, C. B. (1996) Histidine biosynthetic pathway and genes: structure, regulation, and evolution. *Microbiol. Rev.* **60**, 44–69
55. Hawkes, T. R., Thomas, P. G., Edwards, L. S., Rayner, S. J., Wilkinson, K. W., and Rice, D. W. (1995) Purification and characterization of the imidazoleglycerol-phosphate dehydratase of *Saccharomyces cerevisiae* from recombinant *Escherichia coli*. *Biochem. J.* **306**, 385–397
56. Fort, P., Kajava, A. V., Delsuc, F., and Coux, O. (2015) Evolution of proteasome regulators in eukaryotes. *Genome Biol. Evol.* **7**, 1363–1379
57. Kraut, D. A., Israeli, E., Schrader, E. K., Patil, A., Nakai, K., Navanet, D., Inobe, T., and Matouschek, A. (2012) Sequence- and species-dependence of proteasomal processivity. *ACS Chem. Biol.* **7**, 1444–1453
58. Wilkinson, C. R., Seeger, M., Hartmann-Petersen, R., Stone, M., Wallace, M., Semple, C., and Gordon, C. (2001) Proteins containing the UBA domain are able to bind to multi-ubiquitin chains. *Nat. Cell Biol.* **3**, 939–943
59. Schaub, C., Chen, L., Tongaonkar, P., Vega, I., Lambertson, D., Potts, W., and Madura, K. (1998) Rad23 links DNA repair to the ubiquitin/proteasome pathway. *Nature* **391**, 715–718
60. Benjamini, Y., and Hochberg, Y. (1995) Controlling the false discovery rate: a practical and powerful approach to multiple testing. *J. R. Stat. Soc. Series B Stat. Methodol.* **57**, 289–300
61. Kyte, J., and Doolittle, R. F. (1982) A simple method for displaying the hydrophobic character of a protein. *J. Mol. Biol.* **157**, 105–132
62. Vihinen, M., Torkkila, E., and Riikonen, P. (1994) Accuracy of protein flexibility predictions. *Proteins* **19**, 141–149
63. Cilia, E., Pancsa, R., Tompa, P., Lenaerts, T., and Vranken, W. F. (2014) The DynaMine webservice: predicting protein dynamics from sequence. *Nucleic Acids Res.* **42**, W264–W270
64. Cilia, E., Pancsa, R., Tompa, P., Lenaerts, T., and Vranken, W. F. (2013) From protein sequence to dynamics and disorder with DynaMine. *Nat. Commun.* **4**, 2741
65. Buljan, M., Chalancon, G., Eustermann, S., Wagner, G. P., Fuxreiter, M., Bateman, A., and Babu, M. M. (2012) Tissue-specific splicing of disordered segments that embed binding motifs rewires protein interaction networks. *Mol. Cell* **46**, 871–883
66. Weatheritt, R. J., Davey, N. E., and Gibson, T. J. (2012) Linear motifs confer functional diversity onto splice variants. *Nucleic Acids Res.* **40**, 7123–7131
67. Rape, M., Reddy, S. K., and Kirschner, M. W. (2006) The processivity of multiubiquitination by the APC determines the order of substrate degradation. *Cell* **124**, 89–103
68. Williamson, A., Banerjee, S., Zhu, X., Philipp, I., Iavarone, A. T., and

- Rape, M. (2011) Regulation of ubiquitin chain initiation to control the timing of substrate degradation. *Mol. Cell* **42**, 744–757
69. Lu, Y., Wang, W., and Kirschner, M. W. (2015) Specificity of the anaphase-promoting complex: a single-molecule study. *Science* **348**, 1248737
70. Popovic, D., Vucic, D., and Dikic, I. (2014) Ubiquitination in disease pathogenesis and treatment. *Nat. Med.* **20**, 1242–1253
71. Holmberg, C. I., Staniszewski, K. E., Mensah, K. N., Matouschek, A., and Morimoto, R. I. (2004) Inefficient degradation of truncated polyglutamine proteins by the proteasome. *EMBO J.* **23**, 4307–4318
72. Juenemann, K., Schipper-Krom, S., Wiemhoefer, A., Kloss, A., Sanz Sanz, A., and Reits, E. A. (2013) Expanded polyglutamine-containing N-terminal huntingtin fragments are entirely degraded by mammalian proteasomes. *J. Biol. Chem.* **288**, 27068–27084
73. Wang, J., Song, J. J., Franklin, M. C., Kamtekar, S., Im, Y. J., Rho, S. H., Seong, I. S., Lee, C. S., Chung, C. H., and Eom, S. H. (2001) Crystal structures of the HslVU peptidase-ATPase complex reveal an ATP-dependent proteolysis mechanism. *Structure* **9**, 177–184
74. Yamada-Inagawa, T., Okuno, T., Karata, K., Yamanaka, K., and Ogura, T. (2003) Conserved pore residues in the AAA protease FtsH are important for proteolysis and its coupling to ATP hydrolysis. *J. Biol. Chem.* **278**, 50182–50187
75. Hinnerwisch, J., Fenton, W. A., Furtak, K. J., Farr, G. W., and Horwich, A. L. (2005) Loops in the central channel of ClpA chaperone mediate protein binding, unfolding, and translocation. *Cell* **121**, 1029–1041
76. Zhang, F., Wu, Z., Zhang, P., Tian, G., Finley, D., and Shi, Y. (2009) Mechanism of substrate unfolding and translocation by the regulatory particle of the proteasome from *Methanocaldococcus jannaschii*. *Mol. Cell* **34**, 485–496
77. Martin, A., Baker, T. A., and Sauer, R. T. (2008) Pore loops of the AAA⁺ ClpX machine grip substrates to drive translocation and unfolding. *Nat. Struct. Mol. Biol.* **15**, 1147–1151
78. Beckwith, R., Estrin, E., Worden, E. J., and Martin, A. (2013) Reconstitution of the 26S proteasome reveals functional asymmetries in its AAA⁺ unfoldase. *Nat. Struct. Mol. Biol.* **20**, 1164–1172
79. Baker, T. A., and Sauer, R. T. (2012) ClpXP, an ATP-powered unfolding and protein-degradation machine. *Biochim. Biophys. Acta* **1823**, 15–28
80. Iosefson, O., Olivares, A. O., Baker, T. A., and Sauer, R. T. (2015) Dissection of axial-pore loop function during unfolding and translocation by a AAA⁺ proteolytic machine. *Cell Rep.* **12**, 1032–1041
81. Martin, A., Baker, T. A., and Sauer, R. T. (2008) Diverse pore loops of the AAA⁺ ClpX machine mediate unassisted and adaptor-dependent recognition of ssrA-tagged substrates. *Mol. Cell* **29**, 441–450
82. Koga, N., Kameda, T., Okazaki, K.-I., and Takada, S. (2009) Paddling mechanism for the substrate translocation by AAA⁺ motor revealed by multiscale molecular simulations. *Proc. Natl. Acad. Sci. U.S.A.* **106**, 18237–18242
83. Lander, G. C., Estrin, E., Matyskiela, M. E., Bashore, C., Nogales, E., and Martin, A. (2012) Complete subunit architecture of the proteasome regulatory particle. *Nature* **482**, 186–191
84. Matyskiela, M. E., Lander, G. C., and Martin, A. (2013) Conformational switching of the 26S proteasome enables substrate degradation. *Nat. Struct. Mol. Biol.* **20**, 781–788
85. Ślędz, P., Unverdorben, P., Beck, F., Pfeifer, G., Schweitzer, A., Förster, F., and Baumeister, W. (2013) Structure of the 26S proteasome with ATP- γ S bound provides insights into the mechanism of nucleotide-dependent substrate translocation. *Proc. Natl. Acad. Sci. U.S.A.* **110**, 7264–7269
86. Unverdorben, P., Beck, F., Ślędz, P., Schweitzer, A., Pfeifer, G., Plitzko, J. M., Baumeister, W., and Förster, F. (2014) Deep classification of a large cryo-EM dataset defines the conformational landscape of the 26S proteasome. *Proc. Natl. Acad. Sci. U.S.A.* **111**, 5544–5549
87. Kirstein, J., Molière, N., Dougan, D. A., and Turgay, K. (2009) Adapting the machine: adaptor proteins for Hsp100/Clp and AAA⁺ proteases. *Nat. Rev. Microbiol.* **7**, 589–599
88. Flynn, J. M., Neher, S. B., Kim, Y. L., Sauer, R. T., and Baker, T. A. (2003) Proteomic discovery of cellular substrates of the ClpXP protease reveals five classes of ClpX-recognition signals. *Mol. Cell* **11**, 671–683
89. Erales, J., and Coffino, P. (2014) Ubiquitin-independent proteasomal degradation. *Biochim. Biophys. Acta* **1843**, 216–221
90. Wu, H.-Y., Chen, S.-F., Hsieh, J.-Y., Chou, F., Wang, Y.-H., Lin, W.-T., Lee, P.-Y., Yu, Y.-J., Lin, L.-Y., Lin, T.-S., Lin, C.-L., Liu, G.-Y., Tzeng, S.-R., Hung, H.-C., and Chan, N.-L. (2015) Structural basis of antizyme-mediated regulation of polyamine homeostasis. *Proc. Natl. Acad. Sci. U.S.A.* **112**, 11229–11234
91. Chen, H., MacDonald, A., and Coffino, P. (2002) Structural elements of antizymes 1 and 2 are required for proteasomal degradation of ornithine decarboxylase. *J. Biol. Chem.* **277**, 45957–45961
92. Saeki, Y., Isono, E., and Toh-E, A. (2005) Preparation of ubiquitinated substrates by the PY motif-insertion method for monitoring 26S proteasome activity. *Methods Enzymol.* **399**, 215–227
93. Kraut, D. A., and Matouschek, A. (2011) Proteasomal degradation from internal sites favors partial proteolysis via remote domain stabilization. *ACS Chem. Biol.* **6**, 1087–1095
94. Martinez-Fonts, K., and Matouschek, A. (2016) A rapid and versatile method for generating proteins with defined ubiquitin chains. *Biochemistry* **55**, 1898–1908
95. Fleming, J. A., Lightcap, E. S., Sadis, S., Thoroddsen, V., Bulawa, C. E., and Blackman, R. K. (2002) Complementary whole-genome technologies reveal the cellular response to proteasome inhibition by PS-341. *Proc. Natl. Acad. Sci. U.S.A.* **99**, 1461–1466
96. Matsuyama, A., Shirai, A., Yashiroda, Y., Kamata, A., Horinouchi, S., and Yoshida, M. (2004) pDUAL, a multipurpose, multicopy vector capable of chromosomal integration in fission yeast. *Yeast* **21**, 1289–1305
97. Shaner, N. C., Campbell, R. E., Steinbach, P. A., Giepmans, B. N., Palmer, A. E., and Tsien, R. Y. (2004) Improved monomeric red, orange and yellow fluorescent proteins derived from *Discosoma* sp. red fluorescent protein. *Nat. Biotechnol.* **22**, 1567–1572
98. Wilmington, S. R., and Matouschek, A. (2016) An inducible system for rapid degradation of specific cellular proteins using proteasome adaptors. *PLoS ONE* **11**, e0152679
99. Muñoz, V., and Serrano, L. (1994) Elucidating the folding problem of helical peptides using empirical parameters. *Nat. Struct. Biol.* **1**, 399–409
100. Dosztányi, Z., Csizmok, V., Tompa, P., and Simon, I. (2005) IUPred: web server for the prediction of intrinsically unstructured regions of proteins based on estimated energy content. *Bioinformatics* **21**, 3433–3434
101. Rice, P., Longden, I., and Bleasby, A. (2000) EMBOSS: the European Molecular Biology Open Software Suite. *Trends Genet.* **16**, 276–277
102. Wootton, J. C. (1994) Non-globular domains in protein sequences: automated segmentation using complexity measures. *Comput. Chem.* **18**, 269–285
103. Wootton, J. C., and Federhen, S. (1996) Analysis of compositionally biased regions in sequence databases. *Methods Enzymol.* **266**, 554–571
104. Larman, H. B., Zhao, Z., Laserson, U., Li, M. Z., Ciccina, A., Gakidis, M. A., Church, G. M., Kesari, S., Leproust, E. M., Solimini, N. L., and Elledge, S. J. (2011) Autoantigen discovery with a synthetic human peptidome. *Nat. Biotechnol.* **29**, 535–541

Conserved Sequence Preferences Contribute to Substrate Recognition by the Proteasome

Houqing Yu, Amit K. Singh Gautam, Shameika R. Wilmington, Dennis Wylie, Kirby Martinez-Fonts, Grace Kago, Marie Warburton, Sreenivas Chavali, Tomonao Inobe, Ilya J. Finkelstein, M. Madan Babu and Andreas Matouschek

J. Biol. Chem. 2016, 291:14526-14539.

doi: 10.1074/jbc.M116.727578 originally published online May 17, 2016

Access the most updated version of this article at doi: [10.1074/jbc.M116.727578](https://doi.org/10.1074/jbc.M116.727578)

Alerts:

- [When this article is cited](#)
- [When a correction for this article is posted](#)

[Click here](#) to choose from all of JBC's e-mail alerts

Supplemental material:

<http://www.jbc.org/content/suppl/2016/05/17/M116.727578.DC1>

This article cites 104 references, 31 of which can be accessed free at

<http://www.jbc.org/content/291/28/14526.full.html#ref-list-1>